

Plasmonic metal–semiconductor heterostructures for hot-electron-driven photochemistry

Jiawei Huang, Wenxiao Guo, Yue Hu, and Wei David Wei

Plasmonic nanostructures possess broadly tunable optical properties with catalytically active surfaces. They offer new opportunities for achieving efficient solar-to-chemical energy conversion. Plasmonic metal–semiconductor heterostructures have attracted heightened interest due to their capability of generating energetic hot electrons that can be collected to facilitate chemical reactions. In this article, we present a detailed survey of recent examples of plasmonic metal–semiconductor heterostructures for hot-electron-driven photochemistry, including plasmonic metal–oxide, plasmonic metal–two-dimensional materials, and plasmonic metal–metal–organic frameworks. We conclude with a discussion on the remaining challenges in the field and an outlook regarding future opportunities for designing high-performance plasmonic metal–semiconductor heterostructures for photochemistry.

Introduction

The conversion of renewable solar energy to chemical energy represents a promising strategy to reduce current reliance on fossil fuels. The efficient utilization of solar energy in chemical transformations requires photocatalysts to strongly absorb light in the visible region (which constitutes 42% of solar radiation).¹ Plasmonic metal nanoparticles (NPs) (e.g., Au, Ag, and Cu) possess broad absorption across the whole visible region, a quality that attracts tremendous scientific interest in photochemistry.^{2–6} Such capability originates from the unique optical property called surface plasmon resonance (SPR),⁷ which can be understood as a coherent oscillation of conduction electrons induced by incident light when the frequency of the light matches the intrinsic resonant frequency of the plasmonic metal NPs.^{8,9} The SPR excitation consequently generates an intense localized electromagnetic (EM) field on plasmonic metal NPs, which in turn amplifies the absorption of light at the same frequency.^{8,9}

Upon SPR excitation, the oscillation of conduction electrons quickly decays to generate hot electrons that play essential roles in prompting photochemical reactions.^{2,3} However, it is challenging for these hot electrons to directly drive chemical reactions on the surface of plasmonic metal NPs as there is a significant mismatch between the lifetimes of hot electrons (femtoseconds to nanoseconds) and the time scale of chemical

reactions (microseconds to seconds).^{2,3} In addition, the chemical inertness of plasmonic noble metals prevents them from facilitating a wider range of reactions.¹⁰ The development of plasmonic metal–semiconductor heterostructures offers a strategy for resolving these two limitations. In these heterostructures, Schottky barriers are formed at the plasmonic metal–semiconductor interface, which prolong the lifetime of hot electrons into the time scale of chemical reactions once they are transferred into semiconductors.^{11,12} Meanwhile, surface defects on semiconductors, such as oxygen vacancies, provide additional active sites to promote chemical reactions by simultaneously functioning as trapping sites for hot electrons and adsorption sites of reactant molecules.^{13,14}

This article focuses on recent progress in using plasmonic metal–semiconductor heterostructures for hot-electron-driven photochemistry. We begin by summarizing the application of plasmonic heterostructures using oxides as substrates in photochemistry, including the most commonly used modification strategies for improving the performance of these heterostructures. Subsequent sections describe other types of semiconductors, such as two-dimensional (2D) materials and metal–organic frameworks (MOFs), as supports for plasmonic metal NPs. The article concludes with an outlook on potential directions in designing high-performing plasmonic metal–semiconductor heterostructures for hot-carrier-driven photochemistry.

Jiawei Huang, Department of Chemistry, University of Florida, USA; jiawei@chem.ufl.edu
Wenxiao Guo, Department of Chemistry, University of Florida, USA; grandpacomp@chem.ufl.edu
Yue Hu, Department of Chemistry, University of Florida, USA; hulilis@chem.ufl.edu
Wei David Wei, Department of Chemistry, University of Florida, USA; wei@chem.ufl.edu
doi:10.1557/mrs.2019.292

Hot-electron-driven photochemistry on plasmonic metal-oxide heterostructures

Plasmonic metal-oxide heterostructures have been extensively utilized for hot-electron-driven photochemistry due to their interfacial Schottky barrier that enables carrier separation as well as additional active sites provided by oxides for photochemical reactions. The addition of Au NPs onto TiO_2 , ZnO , and CeO_2 has been employed to successfully drive hydrogen production,^{11,15} CO_2 reduction,^{16,17} and organic transformations.¹⁸⁻²⁰ Recently, numerous modifications have been applied to plasmonic metal-oxide heterostructures to further improve their performance in hot-electron-driven photochemistry.

Modifications on plasmonic metal NPs

Altering the size of plasmonic metal NPs has enabled catalytic enhancement in hot-electron photochemistry. Wei and co-workers¹² found that Au/TiO_2 heterostructures with large Au NPs 67 nm in diameter outperformed those with small 4.4-nm Au NPs in H_2 production. The authors attributed this size-dependent activity difference to a larger optical absorption cross section of 67-nm Au NPs compared with that of the 4.4 nm ones, resulting in the generation of more hot electrons to transfer into the conduction band (CB) of TiO_2 for H_2 production. Similarly, Pradhan and co-workers²¹ demonstrated that increasing the size of Au NPs on SnS improved the photocatalytic activity of methylene blue reduction.

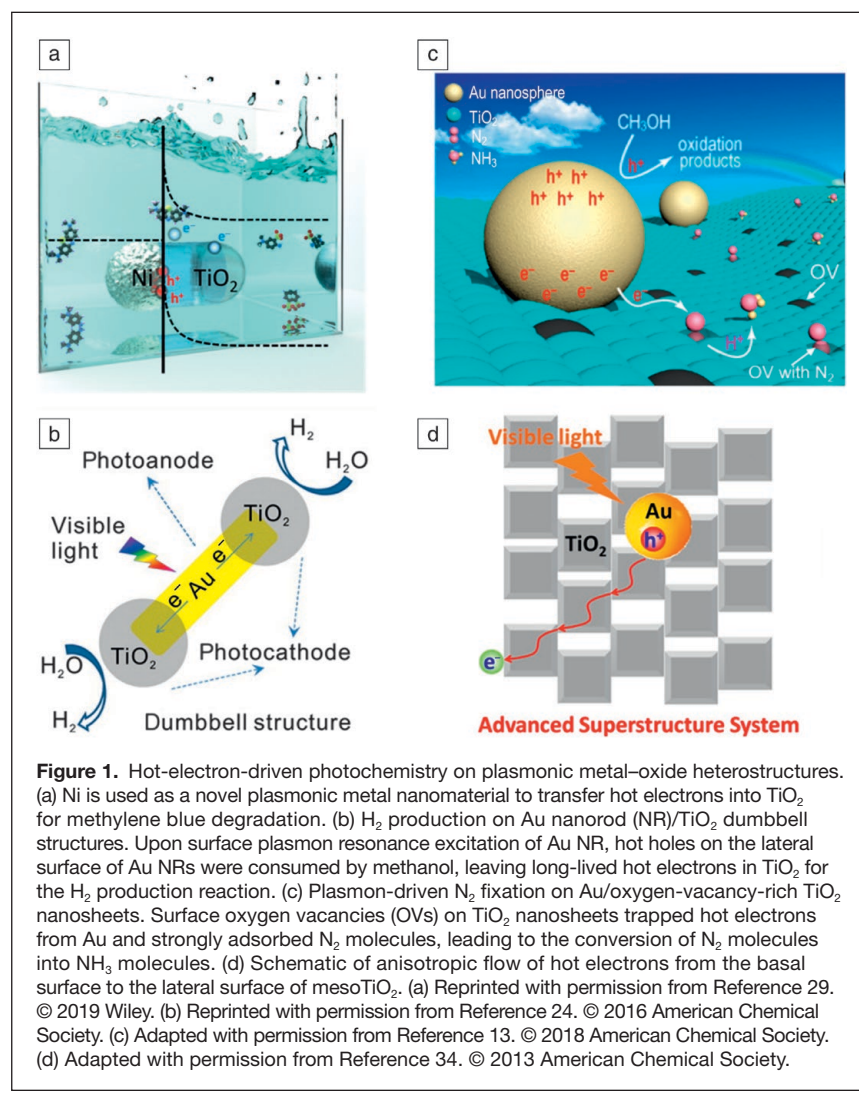
Distinct morphologies of plasmonic metal NPs have also been developed for photochemical reactions. Au nanorods (NRs) with a significantly broadened absorption in the visible and near-infrared (NIR) region are able to drive photochemistry using low-energy photons.²²⁻²⁵ For instance, Ye and co-workers²² loaded Au NRs onto TiO_2 and achieved the oxidation of 2-propanol using visible-NIR light. Majima and co-workers²³ utilized Au NRs as photosensitizers and achieved H_2 production on Au NR/ $\text{La}_2\text{Ti}_2\text{O}_7$ heterostructures under visible-NIR irradiation. Au nanocubes and nanocages with flat surfaces ensure face-to-face interfacial contact with oxides, and this well-defined interfacial contact benefits hot-electron transfer from Au into oxides.²⁶ Xiong and co-workers²⁶ integrated Au nanocubes and nanocages onto TiO_2 nanosheets and detected higher activity of H_2 production compared to that on Au NR/ TiO_2 nanosheet heterostructures, in which the smaller contact area between the curved Au NR surface and TiO_2 nanosheets limited the efficiency of interfacial electron transfer. Moreover, Au nanostars were found to possess an intense EM field at their spikes.²⁷ Upon loading onto TiO_2 , this intense EM field promoted interfacial

hot-electron transfer from the Au nanostars into TiO_2 , resulting in a higher activity of rhodamine B degradation than that on TiO_2 -supported Au nanospheres or NRs.

Recently, great efforts have been made in utilizing earth-abundant and inexpensive metal NPs to substitute noble plasmonic metal NPs. Halas and co-workers²⁸ observed the plasmonic properties of Al and successfully achieved a hot-electron-driven reverse water-gas shift reaction using plasmonic Al/ Cu_2O heterostructures. Later, Wei and co-workers²⁹ discovered that Ni also exhibited plasmonic absorption in the visible range and the plasmon excitation of Ni induced the transfer of hot electrons into TiO_2 for driving methylene blue degradation (Figure 1a). Additionally, Pd and Cu have also been reported as promising plasmonic nanomaterials for chemical reactions by constructing heterostructures with oxides.^{30,31}

Modifications on oxides

Site-selective overgrowth of oxides as a means to manipulate the spatial arrangement of oxides with respect to plasmonic metal NPs has attracted substantial research interest. One advantage



of this site-selective overgrowth is allowing both hot electrons and hot holes to be freely accessed by reactant molecules.^{24,25} A study by Stucky and co-workers²⁴ selectively fabricated TiO₂ at the two ends of Au NRs, in which hot holes on the lateral surface of Au NRs were consumed by methanol and long-lived hot electrons accumulated in TiO₂ enabling the H₂ production reaction (Figure 1b). CeO₂ was also grown onto the two ends of Au NRs for N₂ fixation.²⁵ A 6.2-fold higher yield of ammonia formation was detected as compared to Au NR/CeO₂ core-shell nanostructures, in which hot holes were blocked by the CeO₂ shell and led to recombination with hot electrons. Another advantage of controlling oxides at specific sites of plasmonic metal NPs is to facilitate hot-electron transfer at the plasmonic metal–oxide interface.³² For example, the attachment of Cu₂O at the high-curvature vertices of hexoctahedral Au NPs took advantage of an intense EM field at the vertices to promote hot-electron transfer into Cu₂O for improving H₂ production.³²

Introducing active sites onto oxides has been extensively investigated as a strategy to further increase the activity of photochemical reactions. Yu and co-workers¹³ created oxygen vacancies on TiO₂ nanosheets to both trap hot electrons from Au NPs and strongly adsorb N₂ molecules (Figure 1c), resulting in the conversion of N₂ molecules into ammonia with the apparent quantum efficiency of 0.82% under 550-nm irradiation. Another method of creating active sites is to integrate secondary materials. Depositing Pt NPs onto Au/TiO₂ heterostructures has been widely used for promoting the H₂ production reaction.^{33–35} Other metal NPs, such as Ag and Pd, have also been employed as active sites on Au/TiO₂ heterostructures.^{19,26,33} Gong and co-workers¹⁴ deposited a thin amorphous TiO₂ layer on Au/TiO₂ heterostructures and discovered that this amorphous TiO₂ layer provided oxygen vacancies to facilitate hot-electron-driven N₂ fixation.

The development of oxides with different intrinsic electronic properties allows for the anisotropic flow of hot electrons to facilitate carrier separation. Majima and co-workers³⁴ deposited Au NPs on the basal surface of anatase TiO₂ mesocrystal (MesoTiO₂) and found that hot electrons originally transferred from Au onto the basal surface further migrated to the lateral surface due to different electron affinities between these two surfaces (Figure 1d). Efficient electron–hole separation on Au/MesoTiO₂ heterostructures resulted in more than an order of magnitude higher activity of organic molecule degradation than on conventional Au/TiO₂ heterostructures. Later, they deposited Au NRs onto La₂Ti₂O₇ with (010) and (012) facets.²³ Since the (010) facet had a more negative CB minimum potential (−0.72 eV versus NHE) than that of the (012) facet (−0.52 eV versus NHE), hot electrons transferred to the (010) facet would further diffuse to the (012) facet, suppressing the electron–hole recombination and leading to enhancement in H₂ production.

Hot-electron-driven photochemistry on plasmonic metal–2D semiconductor heterostructures

In recent years, combining plasmonic metal NPs with thin-layer 2D semiconductors has attracted increasing interest in

hot-electron photochemistry.^{36–41} The electronic structure of 2D semiconductors is usually tunable by controlling their thickness or phase,^{42,43} which makes it possible to design suitable Schottky barriers between 2D semiconductors and plasmonic metal NPs for the efficient utilization of hot electrons. Meanwhile, their large surface area provides more active sites for targeting reactions.^{42,43} Both properties predict the great potential of plasmonic metal–2D semiconductor heterostructures as photocatalysts for chemical reactions.

A 2D molybdenum disulfide (MoS₂) nanosheet, which is known for its high activity for the H₂ evolution reaction,^{44,45} is one of the most promising candidates for constructing plasmonic metal–2D semiconductor photocatalysts. For instance, Au NRs with a SPR peak at around 810 nm were deposited on chemically exfoliated MoS₂ nanosheets.³⁷ Upon SPR excitation of the Au NRs, the transfer of hot electrons from Au NRs into MoS₂ elevated the Fermi level of MoS₂ to the energy level of the H⁺/H₂ redox pair, resulting in enhanced activity of MoS₂ for the electrochemical H₂ evolution reaction (Figure 2a). Similar improvement in the activity of the H₂ evolution reaction has also been reported on MoS₂ nanosheets decorated with Au nanotriangles.³⁶ Recently, a study observed fourfold enhancement of the plasmon-driven H₂ evolution reaction on Au/MoS₂ heterostructures by introducing a Pd layer between the Au and MoS₂.³⁸ In these Au/Pd/MoS₂ heterostructures, the lattice mismatch between Pd and MoS₂ induced a phase variation of MoS₂ from 2H (the semiconducting phase of MoS₂) to 1T (the metallic phase of MoS₂), known to have lower electronic resistance and provide more active sites for the H₂ evolution reaction.⁴⁶ As a result, the construction of such a Au/Pd/MoS₂ heterostructure contributed to a more efficient hot-electron transfer from Au to MoS₂, eventually leading to higher activity of the H₂ evolution reaction (Figure 2b).

Graphene-like structures such as reduced graphene oxide (rGO) and graphitic carbon nitride (g-C₃N₄) exhibit high electronic conductivity due to their large conjugated π system, which is beneficial for facilitating the separation of carriers in photochemistry.^{47,48} Majima and co-workers³⁹ fabricated rGO nanosheets decorated with Au nanotriangles and Pt nanoframes as photocatalysts for the H₂ evolution reaction, in which hot electrons generated in Au efficiently transferred to rGO and further transported to catalytically active Pt nanoframes. Similarly, g-C₃N₄ substrates with both Au and Pt nanostructures co-deposited were also reported as photocatalysts for chemical reactions, including the H₂ evolution reaction and tetracycline hydrochloride degradation.^{40,41}

Hot-electron-driven photochemistry on plasmonic metal/MOF heterostructures

Due to their high surface-to-volume ratio, tunable porosities, and adjustable internal surface properties, MOFs are known for the outstanding capability for capturing reactant molecules.⁴⁹ Meanwhile, multiple options of metal ions (or clusters) and organic ligands enable the fabrication of different types of MOFs with distinct catalytic properties.^{50,51}

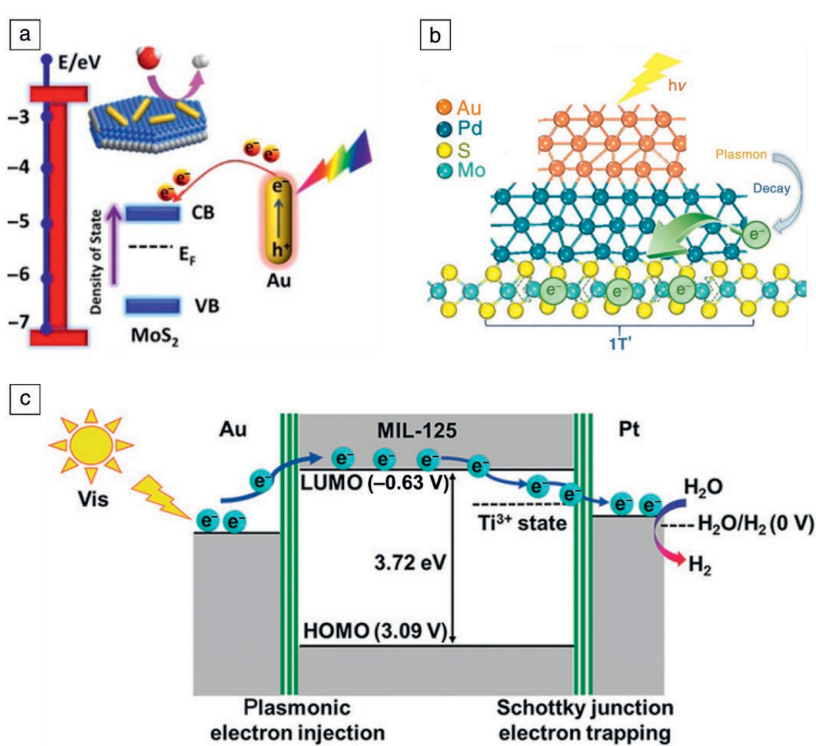


Figure 2. Hot-electron-driven photochemistry on other plasmonic metal–semiconductor heterostructures. (a) H₂ evolution reaction on Au NR/MoS₂ heterostructures. Hot electrons excited in Au NRs transferred to the CB of MoS₂ driving the H₂ evolution reaction. (b) Efficient hot-electron transfer from Au/Pd to 1T phase MoS₂ (the metallic phase of MoS₂) for the H₂ evolution reaction. (c) H₂ production on Au NR/MIL-125/Pt heterostructures. Hot electrons transferred from Au into Ti³⁺ states of MIL-125 and further diffused into Pt to achieve the H₂ production reaction. (a) Reprinted with permission from Reference 37. © 2015 American Chemical Society. (b) Reprinted with permission from Reference 46. 2019 American Chemical Society. (c) Reprinted with permission from Reference 52. © 2018 Wiley. Note: CB, conduction band; VB, valence band; HOMO, highest occupied molecular orbital; LUMO, lowest unoccupied molecular orbital.

These advantages make plasmonic metal–MOF heterostructures catalytically active for photochemical reactions, such as the H₂ production reaction^{52,53} and the reverse water–gas shift reaction.⁵⁴

Jiang and co-workers⁵² assembled Au NRs onto Pt-decorated MIL-125 (a TiO₂/1,4-benzenedicarboxylate (bdc) MOF) as photocatalysts for the H₂ production reaction. The transfer of hot electrons from Au to Ti centers of MIL-125 and subsequently Pt sites efficiently suppressed the recombination of carriers, facilitating the production of H₂ molecules on Pt sites (Figure 2c). Similarly, Au NR-incorporated CoFe-MOF nanosheets were developed, in which hot electrons were transferred from Au NRs to Co centers to boost the activity of the H₂ evolution reaction.⁵³ Recently, Halas and co-workers⁵⁴ reported the use of a novel plasmonic metal, Al nanocrystal (NC), as the core to grow Al NC@MIL-53(Al) core–shell structures for the plasmon-driven hydrogen-deuterium (H-D) exchange. These Al NC@MIL-53(Al) core–shell structures were also catalytically active for the plasmon-driven reverse water–gas shift reaction, which showed a higher selectivity toward CO molecules rather than the side

product (CH₄) when compared with the thermally driven pathway.⁵⁴

Conclusion

A wide range of plasmonic metal–semiconductor heterostructures have been developed to drive hot-electron photochemistry. Further improvement in the efficiency of chemical reactions requires the use of semiconductors that enable the more efficient accumulation of hot electrons. Metal halide perovskite has been proposed as a promising candidate. Xiao and co-workers⁵⁵ observed that the quantum efficiency of interfacial hot-electron transfer in Ag/CsPbBr₃ heterostructures reached 50 ± 18%, higher than the 40% in Au/TiO₂ heterostructures.⁵⁶ Meanwhile, the long diffusion lengths of carriers in metal halide perovskites would benefit electron–hole separation,⁵⁷ allowing more hot electrons to be available for participating in chemical reactions. However, the fast decomposition of metal–halide perovskites upon exposure to moisture, oxygen molecules, and light limits their applications in photochemistry.⁵⁸ Recently, studies have been reported to modify metal–halide perovskites to improve their stability. For instance, introducing a larger organic cation into inorganic metal halide perovskites induces morphology transformation from 3D into 2D structures. Similarly, using less acidic cations enabled the stability enhancement of metal halide perovskites.⁵⁸ This progress supports the potential of using plasmonic metal–metal halide perovskite heterostructures for photochemical reactions.

In addition to hot electrons, there is increased research interest in the utilization of hot holes for oxidation reactions. For example, Li and co-workers⁵⁹ used hot holes accumulated at the Au–TiO₂ interface for water oxidation reaction; however, the insufficient amount of hot holes at active sites limited the overall yield of O₂ molecules. Therefore, the strategies of efficiently accumulating hot holes on plasmonic metal–semiconductor heterostructures need to be explored. Atwater and co-workers⁶⁰ utilized the interfacial Schottky barrier between Au NPs and p-GaN to prevent the relaxation of hot holes back to Au NPs once they were transferred to p-GaN. Meanwhile, introducing a hole-storing material onto plasmonic metal–semiconductor heterostructures has also been developed for the accumulation of hot holes.^{35,61} However, effects of hole-storing materials on the activity of hot-hole-driven oxidation reactions were found to be sensitive to their spatial distributions on plasmonic metal–semiconductor heterostructures. For instance, Moskovits and co-workers³⁵ attached cobalt-based oxygen evolution catalysts (Co-OEC) on the Au surface of Au nanorod/TiO₂ heterostructures, in

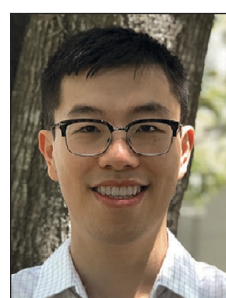
which Co-OEC could trap hot holes and promote the water oxidation reaction. In contrast, Li and co-workers⁵⁹ observed that the deposition of MnO_x (a commonly used electrocatalyst of water oxidation) near the Au-TiO₂ interface suppressed the activity of water oxidation. Therefore, insights into the importance of spatial distribution of hole-storing materials in determining plasmonic photochemistry would greatly assist in the optimization of photochemical reactions on plasmonic metal-semiconductor heterostructures.

Acknowledgments

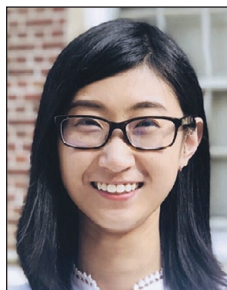
This work is supported by the National Science Foundation under Grant Nos. CHE-1808539 and DMR-1352328. W.G. acknowledges the support of a graduate school fellowship from the University of Florida and the US Department of Energy Science Graduate Student Research Award.

References

1. Reference Solar Spectral Irradiance: Air Mass 1.5," <http://rredc.Nrel.gov/solar/spectra/am1.5> (accessed October 23, 2017).
2. Y. Zhang, S. He, W. Guo, Y. Hu, J. Huang, J.R. Mulcahy, W.D. Wei, *Chem. Rev.* **118**, 2927 (2018).
3. M.L. Brongersma, N.J. Halas, P. Nordlander, *Nat. Nanotechnol.* **10**, 25 (2015).
4. S. Linic, U. Aslam, C. Boerigter, M. Morabito, *Nat. Mater.* **14**, 567 (2015).
5. U. Aslam, V.G. Rao, S. Chavez, S. Linic, *Nat. Catal.* **1**, 656 (2018).
6. M.J. Kale, T. Avanesian, P. Christopher, *ACS Catal.* **4**, 116 (2014).
7. V. Giannini, A.I. Fernández-Domínguez, S.C. Heck, S.A. Maier, *Chem. Rev.* **111**, 3888 (2011).
8. K.A. Willets, R.P. Van Duyne, *Annu. Rev. Phys. Chem.* **58**, 267 (2007).
9. R.L. Giesecking, M.A. Ratner, G.C. Schatz, *ACS Symp. Ser.* **1245** (1), 1 (2016).
10. B. Hammer, J.K. Norskov, *Nature* **376**, 238 (1995).
11. J.S. Duchene, B.C. Sweeny, A.C. Johnston-Peck, D. Su, E.A. Stach, W.D. Wei, *Angew. Chem. Int. Ed. Engl.* **53**, 7887 (2014).
12. K. Qian, B.C. Sweeny, A.C. Johnston-Peck, W. Niu, J.O. Graham, J.S. Duchene, J. Qiu, Y.C. Wang, M.H. Engelhard, D. Su, E.A. Stach, W.D. Wei, *J. Am. Chem. Soc.* **136**, 9842 (2014).
13. J. Yang, Y. Guo, R. Jiang, F. Qin, H. Zhang, W. Lu, J. Wang, J.C. Yu, *J. Am. Chem. Soc.* **140**, 8497 (2018).
14. C. Li, T. Wang, Z.J. Zhao, W. Yang, J.F. Li, A. Li, Z. Yang, G.A. Ozin, J. Gong, *Angew. Chem. Int. Ed. Engl.* **57**, 5278 (2018).
15. J.B. Priebe, M. Karnahl, H. Junge, M. Beller, D. Hollmann, A. Brückner, *Angew. Chem. Int. Ed. Engl.* **52**, 11420 (2013).
16. W. Hou, W.H. Hung, P. Pavaskar, A. Goeppert, M. Aykol, S.B. Cronin, *ACS Catal.* **1**, 929 (2011).
17. L. Collado, A. Reynal, J.M. Coronado, D.P. Serrano, J.R. Durrant, V.A. De la Peña O'Shea, *Appl. Catal. B* **178**, 177 (2015).
18. D. Tsukamoto, Y. Shiraishi, Y. Sugano, S. Ichikawa, S. Tanaka, T. Hirai, *J. Am. Chem. Soc.* **134**, 6309 (2012).
19. A. Tanaka, Y. Nishino, S. Sakaguchi, T. Yoshikawa, K. Imamura, K. Hashimoto, H. Kominami, *Chem. Commun.* **49**, 2551 (2013).
20. Q. Zhang, X. Jin, Z. Xu, J. Zhang, U.F. Rendón, L. Razzari, M. Chaker, D. Ma, *J. Phys. Chem. Lett.* **9**, 5317 (2018).
21. B.K. Patra, A.K. Guria, A. Dutta, A. Shit, N. Pradhan, *Chem. Mater.* **26**, 7194 (2014).
22. L. Liu, S. Ouyang, J. Ye, *Angew. Chem. Int. Ed. Engl.* **52**, 6689 (2013).
23. X. Cai, M. Zhu, O.A. Elbanna, M. Fujitsuka, S. Kim, L. Mao, J. Zhang, T. Majima, *ACS Catal.* **8**, 122 (2018).
24. B. Wu, D. Liu, S. Mubeen, T.T. Chuong, M. Moskovits, G.D. Stucky, *J. Am. Chem. Soc.* **138**, 1114 (2016).
25. H. Jia, A. Du, H. Zhang, J. Yang, R. Jiang, J. Wang, C.Y. Zhang, *J. Am. Chem. Soc.* **141**, 5083 (2019).
26. W. Jiang, S. Bai, L. Wang, X. Wang, L. Yang, Y. Li, D. Liu, X. Wang, Z. Li, J. Jiang, Y. Xiong, *Small* **12**, 1640 (2016).
27. A. Sousa-Castillo, M. Comesáñ-Hermo, B. Rodríguez-González, M. Pérez-Lorenzo, Z. Wang, X.T. Kong, A.O. Govorov, M.A. Correa-Duarte, *J. Phys. Chem. C* **120**, 11690 (2016).
28. H. Robatjazi, H. Zhao, D.F. Swearer, N.J. Hogan, L. Zhou, A. Alabastri, M.J. McClain, P. Nordlander, N.J. Halas, *Nat. Commun.* **8**, (2017).
29. S. He, J. Huang, J.L. Goodsell, A. Angerhofer, W.D. Wei, *Angew. Chem. Int. Ed. Engl.* **58**, 6038 (2019).
30. J. Zou, Z. Si, Y. Cao, R. Ran, X. Wu, D. Weng, *J. Phys. Chem. C* **120**, 29116 (2016).
31. E. Liu, L. Qi, J. Bian, Y. Chen, X. Hu, J. Fan, H. Liu, C. Zhu, Q. Wang, *Mater. Res. Bull.* **68**, 203 (2015).
32. J.W. Hong, D.H. Wi, S.U. Lee, S.W. Han, *J. Am. Chem. Soc.* **138**, 15766 (2016).
33. A. Tanaka, S. Sakaguchi, K. Hashimoto, H. Kominami, *ACS Catal.* **3**, 79 (2013).
34. Z. Bian, T. Tachikawa, P. Zhang, M. Fujitsuka, T. Majima, *J. Am. Chem. Soc.* **136**, 458 (2014).
35. S. Mubeen, J. Lee, N. Singh, S. Krämer, G.D. Stucky, M. Moskovits, *Nat. Nanotechnol.* **8**, 247 (2013).
36. P. Zhang, M. Fujitsuka, T. Majima, *Nanoscale* **9**, 1520 (2017).
37. Y. Shi, J. Wang, C. Wang, T.T. Zhai, W.J. Bao, J.J. Xu, X.H. Xia, H.Y. Chen, *J. Am. Chem. Soc.* **137**, 7365 (2015).
38. B. Shang, X. Cui, L. Jiao, K. Qi, Y. Wang, J. Fan, Y. Yue, H. Wang, Q. Bao, X. Fan, S. Wei, W. Song, Z. Cheng, S. Guo, W. Zheng, *Nano Lett.* **19**, 2758 (2019).
39. Z. Lou, M. Fujitsuka, T. Majima, *J. Phys. Chem. Lett.* **8**, 844 (2017).
40. L. Zhang, N. Ding, L. Lou, K. Iwasaki, H. Wu, Y. Luo, D. Li, K. Nakata, A. Fujishima, Q. Meng, *Adv. Funct. Mater.* **29**, 1 (2019).
41. J. Xue, S. Ma, Y. Zhou, Z. Zhang, M. He, *ACS Appl. Mater. Interfaces* **7**, 9630 (2015).
42. H. Jin, C. Guo, X. Liu, J. Liu, A. Vasileff, Y. Jiao, Y. Zheng, S.Z. Qiao, *Chem. Rev.* **118**, 6337 (2018).
43. W.J. Ong, L.L. Tan, Y.H. Ng, S.T. Yong, S.P. Chai, *Chem. Rev.* **116**, 7159 (2016).
44. C. Liu, D. Kong, P.C. Hsu, H. Yuan, H.W. Lee, Y. Liu, H. Wang, S. Wang, K. Yan, D. Lin, P.A. Maraccini, K.M. Parker, A.B. Boehm, Y. Cui, *Nat. Nanotechnol.* **11**, 1098 (2016).
45. D. Voiry, R. Fullon, J. Yang, C. de Carvalho Castro e Silva, R. Kappera, I. Bozkurt, D. Kaplan, M.J. Lagos, P.E. Batson, G. Gupta, A.D. Mohite, L. Dong, D. Er, V.B. Shenoy, T. Asefa, M. Chhowalla, *Nat. Mater.* **15**, 1003 (2016).
46. J. Zhang, J. Wu, H. Guo, W. Chen, J. Yuan, U. Martinez, G. Gupta, A. Mohite, P.M. Ajayan, J. Lou, *Adv. Mater.* **29**, 1 (2017).
47. M.E. Khan, M.M. Khan, M.H. Cho, *Nanoscale* **10**, 9427 (2018).
48. Q. Han, N. Chen, J. Zhang, L. Qu, *Mater. Horiz.* **4**, 832 (2017).
49. H.C. Zhou, J.R. Long, O.M. Yaghi, *Chem. Rev.* **112**, 673 (2012).
50. A. Corma, H. Garcia, F.X. Llabrés i Xamena, *Chem. Rev.* **110**, 4606 (2010).
51. L. Zhu, X.Q. Liu, H.L. Jiang, L.B. Sun, *Chem. Rev.* **117**, 8129 (2017).
52. J.D. Xiao, L. Han, J. Luo, S.H. Yu, H.L. Jiang, *Angew. Chem. Int. Ed. Engl.* **57**, 1103 (2018).
53. H.-L. Jiang, S.-S. Wang, L. Jiao, Y. Qian, W.-C. Hu, G.-Y. Xu, C. Wang, *Angew. Chem. Int. Ed. Engl.* **58**, 1 (2019).
54. H. Robatjazi, D. Weinberg, D.F. Swearer, C. Jacobson, M. Zhang, S. Tian, L. Zhou, P. Nordlander, N.J. Halas, *Sci. Adv.* **5**, 5340 (2019).
55. X. Huang, H. Li, C. Zhang, S. Tan, Z. Chen, L. Chen, Z. Lu, X. Wang, M. Xiao, *Nat. Commun.* **10**, 1 (2019).
56. A. Furube, L. Du, K. Hara, R. Katoh, M. Tachiya, *J. Am. Chem. Soc.* **129**, 14852 (2007).
57. J.S. Manser, J.A. Christians, P.V. Kamat, *Chem. Rev.* **116**, 12956 (2016).
58. C.C. Boyd, R. Cheacharoen, T. Leijtens, M.D. McGehee, *Chem. Rev.* **119**, 3418 (2019).
59. S. Wang, Y. Gao, S. Miao, T. Liu, L. Mu, R. Li, F. Fan, C. Li, *J. Am. Chem. Soc.* **139**, 11771 (2017).
60. J.S. Duchene, G. Tagliabue, A.J. Welch, W.H. Cheng, H.A. Atwater, *Nano Lett.* **18**, 2545 (2018).
61. S.F. Hung, F.X. Xiao, Y.Y. Hsu, N.T. Suen, H. Bin Yang, H.M. Chen, B. Liu, *Adv. Energy Mater.* **6**, 1 (2016). □



Jiawei Huang is a doctoral candidate in physical chemistry at the University of Florida. He received his bachelor's degree in engineering from Xi'an Jiaotong University, China, in 2015. His research focuses on *in situ* observation of interfacial hot-carrier transfer within plasmonic metal-semiconductor heterostructures for photochemistry. Huang can be reached by email at jiawei.huang@chem.ufl.edu.



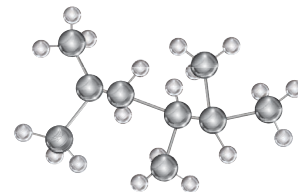
Wenxiao Guo is a doctoral candidate in physical chemistry at the University of Florida. She received her BS degree in chemical technology at The Hong Kong Polytechnic University, Hong Kong, in 2014. Her research focuses on controlling the photocatalytic activity of plasmonic metal nanostructures with functional surfactants and adsorbates. Guo can be reached by email at grandpacomp@chem.ufl.edu.



Wei David Wei is an associate professor in the Department of Chemistry at the University of Florida. He received his PhD degree from The University of Texas at Austin in 2005, and completed postdoctoral research at Northwestern University. His research interests include the novel electronic and optical properties of metallic and semiconductor nanomaterials and their applications in solar-energy harvesting, conversion, and storage; visible-light photocatalysis; and chemical and biological detection. Wei can be reached by email at wei@chem.ufl.edu.



Yue Hu is a doctoral candidate in physical chemistry at the University of Florida. She received her BS degree in materials science at Sun Yat-Sen University, China, in 2015. Her research focuses on developing functional surfactants to manipulate the catalytic properties of plasmonic nanostructures. Hu can be reached by email at hulilis@chem.ufl.edu.










MRS MEMBERSHIP Discounts for Developing Countries

Interdisciplinary. Broadly Inclusive. Egalitarian.

For the Materials Research Society, these words are at the core of our mission, vision and values—to *build a dynamic, interactive, global community of materials researchers*.

To better serve students and professionals from all technical and economic sectors of the worldwide materials community, those **individuals working or studying in developing countries*** are **eligible for discounted membership**.

Funded by the Materials Research Society Foundation, these memberships enable materials scientists to connect with colleagues from around the world, and contribute to, and benefit from, the Society's programs.

2020 Membership Rates (US dollars)	Regular Rate	Lower- and Middle-Income Countries*	Low-Income Countries*
Professional Membership	\$135	\$63	\$30
Student Membership	\$35	FREE	FREE

*Countries are based on those defined as Low-Income or Lower-Middle-Income Economies by the World Bank. For a complete list of qualifying countries, visit mrs.org/dev-countries-member.

mrs.org/dev-countries-member



MATERIALS RESEARCH SOCIETY
FOUNDATION